Korean J. Chem. Eng., 39(2), 398-407 (2022)
DOI: 10.1007/s11814-021-1028-5

pISSN: 0256-1115
eISSN: 1975-7220

Ultrasound-negative pressure cavitation extraction of paclitaxel from *Taxus chinensis*

Hye-Su Min, Hak-Gyun Kim, and Jin-Hyun Kim†

Department of Chemical Engineering, Kongju National University, Cheonan 31080, Korea
(*Received 26 September 2021 • Revised 21 November 2021 • Accepted 29 November 2021*)

Abstract−An ultrasound-negative pressure cavitation extraction method was developed to remarkably improve the recovery efficiency of paclitaxel from *Taxus chinensis*. The paclitaxel yield was 94-100% through ultrasound-negative pressure cavitation extraction with an extraction time of 3 to 8 min. In particular, most paclitaxel could be recovered within 3 min of extraction at ultrasonic power of 380 W/negative pressure of −260 mmHg. Observation of the biomass surface with SEM before and after extraction showed that as the ultrasonic power and negative pressure increased, the surface was more disrupted. In addition, a pseudo-second order model was suitable for the kinetic analysis, and intraparticle diffusion played a dominant role in the overall extraction rate according to the intraparticle diffusion model. As the ultrasonic power and negative pressure increased, the extraction rate constant (6.8816-11.6105 mL/mg·min), the effective diffusion coefficient (1.550×10^{-12}-11.528×10^{-12} m^2/s), and the mass transfer coefficient (2.222×10^{-7}-5.149×10^{-7} m/s) increased.

Keywords: Paclitaxel, Cavitation Extraction, Ultrasound-negative Pressure, Kinetics, Effective Diffusion Coefficient, Mass Transfer Coefficient

INTRODUCTION

Paclitaxel (Fig. 1), the most well-known natural-source cancer drug, is extracted from the bark of the Pacific yew tree. It is widely used independently or with other chemotherapeutic agents for treating various types of solid tumors, such as ovarian cancer, breast cancer, head and neck cancers, Kaposi's sarcoma, and non-small cell lung cancer [1,2]. Its demand is expected to grow continuously because its indications are expanding and more treatment methods are being developed [3-5]. Paclitaxel is mainly produced through extraction, semi-synthesis, and plant cell culture [6-8]. Among them, plant cell culture is less affected by external factors, such as climate and the environment, and can stably produce paclitaxel of uniform quality in a bioreactor [8,9].

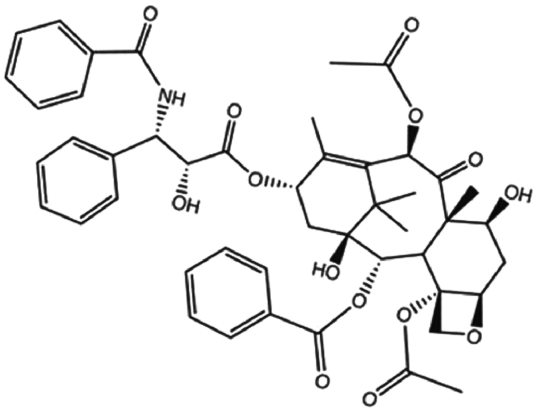

Fig. 1. The chemical structure of paclitaxel.

In the plant cell culture, paclitaxel, a secondary metabolite, is mostly accumulated in plant cells (biomass) [10], and is produced through several stages of extraction and purification [11-13]. From an economic point of view, it is very important to recover paclitaxel in high yields from the biomass. Generally, solvent extraction is widely used to recover paclitaxel, and methanol is known to be the most effective solvent as it requires the least amount of solvent and gives the highest yield [14]. In addition, the paclitaxel recovery rate from biomass was increased by optimizing key process parameters (methanol concentration, biomass/methanol ratio, extraction time, and extraction number) [14]. However, conventional solvent extraction has the disadvantage that considerable organic solvent and processing time are necessary due to several rounds of extraction. Moreover, the solvent toxicity and removal of residual solvents in active pharmaceutical ingredients should be additionally considered. Recently, cavitation-based extraction methods that could more effectively recover active ingredients from biomass have been reported [15-21]. In cavitation, bubbles are formed in a liquid due to a reduction in the liquid's pressure below the saturated vapor pressure, and is mostly generated via ultrasound or negative pressure [20]. Ultrasonic cavitation extraction has been widely used to recover natural substances like polysaccharides from bamboo shoot (*Chimonobambusa quadrangularis*) processing by-products, punicalagin from pomegranate (*Punica granatum*) peels, and oleic acid and linoleic acid from *Osmanthus fragrans* fruit oil [15-19]. Ultrasonic cavitation bubbles go through a process of formation, growth, and collapse, ultimately creating high-speed microjets of liquid, intense localized heating, and high-pressure shock waves. In addition, the hotspots generated through the collapse of the bubbles caused high temperatures and high pressures, resulting in cell wall disruption and the release of compounds into the solvent [22,23]. Negative pressure cavitation also has been widely used to recover

†To whom correspondence should be addressed.
E-mail: jinhyun@kongju.ac.kr

phenolic compounds from *Millettia sercea* roots and bioactive compounds from plant materials [20,21]. When introduced into a liquid-solid system, negative pressure cavitation promotes turbulence, collision, and mass transfer between the extraction solvent and the biomass. Such integrated action decreases bonding strength between the secondary metabolites, plant cell walls, and tissues, resulting in the adequate and rapid release of the secondary metabolites into the extraction solvent [20]. In this study, an ultrasound-negative pressure cavitation extraction method utilizing the synergy of ultrasound combined with negative pressure cavitation was developed for the first time for the effective recovery of paclitaxel from biomass. In addition, the ultrasound-negative pressure cavitation extraction characteristics were quantitatively investigated through a kinetic study of the extraction process. Furthermore, the effective diffusion coefficient as well as the mass transfer coefficient were determined to understand the mass transfer mechanism in ultrasound-negative pressure cavitation extraction. These results could be used effectively in the eco-friendly commercial mass production of the anticancer agent, paclitaxel, via plant cell culture.

MATERIALS AND METHODS

1. Plant Materials

Suspension cells derived from *Taxus chinensis* were cultured at 24 °C under dark conditions while stirring at 150 rpm in modified Gamborg's B5 medium. The plant cell culture medium was replaced with fresh medium every two weeks, and 1-2% (w/v) of maltose was added on the 7th and 21st day of the cell culture to extend the culture period. As an elicitor, 4 μM of $AgNO_3$ was added at the initial stage of culturing [9,24]. After plant cell culturing, the plant biomass was recovered from the culture medium using a decanter (Westfalia, CA150 Clarifying Decanter) and a high-speed centrifuge (α-Laval, BTPX205GD-35CDEEP). The biomass was provided by the Samyang Biopharm Company, South Korea.

2. Extraction Methods

Schematic diagrams of conventional solvent extraction, ultrasonic extraction, negative pressure extraction, and ultrasound-negative pressure cavitation extraction are presented in Fig. 2. In all the extraction processes, the ratio of biomass to methanol was set at 1 : 2 (w/v) and the extraction temperature was ambient (25 °C) to account for the excessive energy consumption when extraction is executed at high temperature. Extraction was executed once, and the stirring speed was set at 500 rpm [15]. When paclitaxel was extracted with ultrasound, the extraction behavior was investigated by varying the ultrasonic power (180, 250, and 380 W) and the extraction time (1, 3, 6, 8, 10, 12, and 20 min) using a 40 kHz ultrasonic bath [(UC-10, Jeiotech, Korea) (180, 250 W) and (JAC-4020, KODO, Korea) (380 W)]. Negative pressure was maintained inside the extractor using a vacuum controller unit (EYELA NVC-3000, Japan) and a diaphragm vacuum pump (EYELA NVP-1000, Japan). Paclitaxel extraction efficiency was investigated by varying the negative pressure (0, −160, and −260 mmHg) and extraction

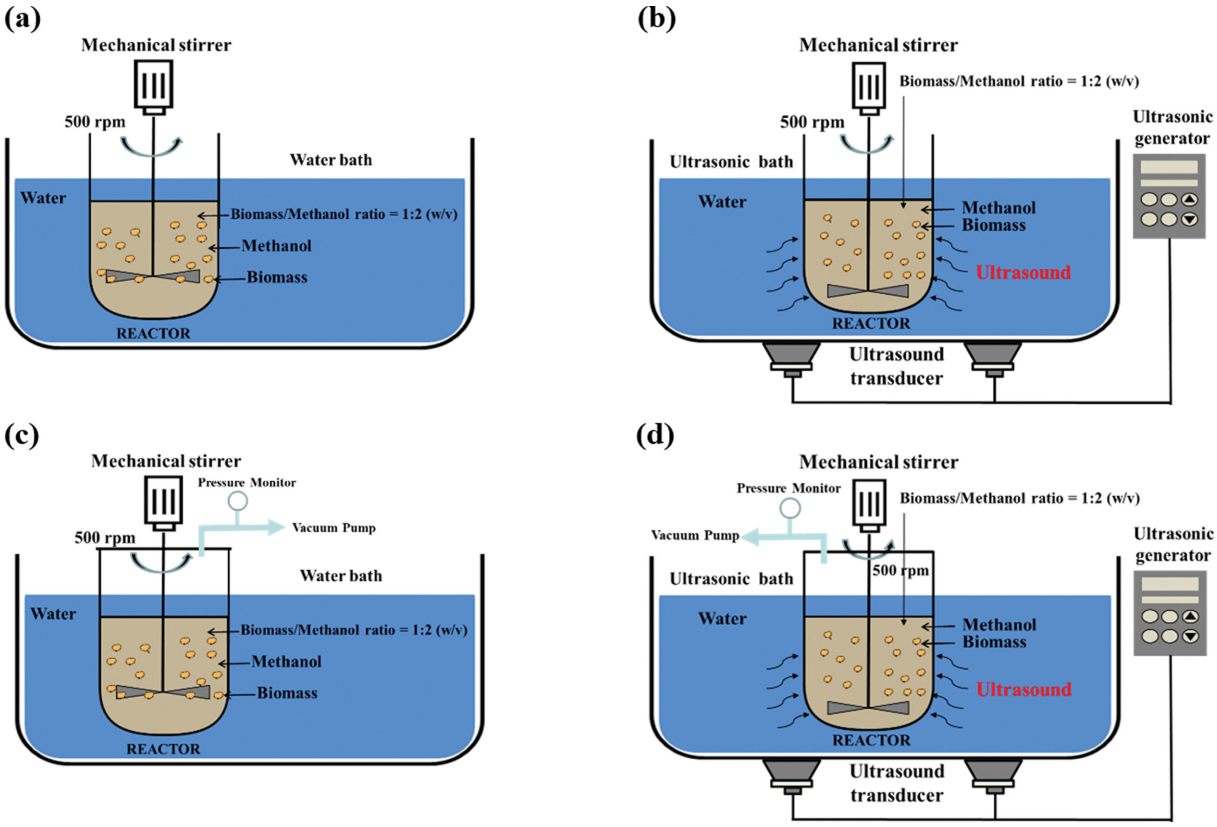

Fig. 2. Schematic diagram of conventional solvent extraction (a), ultrasonic extraction (b), negative pressure extraction (c), ultrasound-negative pressure cavitation extraction (d) for recovery of paclitaxel from biomass.

Table 1. Equations used for parameter estimation in this study

Equation	Parameter	Ref.
Pseudo-first-order model $\ln(C_e-C_t)=\ln C_e-k_1 t$	C_t (mg/mL): concentration of paclitaxel in the suspension at any time C_e (mg/mL): concentration of extracted paclitaxel at equilibrium k_1 (min^{-1}): pseudo-first-order rate constant	[25]
Pseudo-second-order model $\frac{t}{C_t}=\frac{1}{k_2 C_e^2}+\frac{t}{C_e}$ $h=k_2 C_e^2$	k_2 (mL/mg·min): pseudo-second-order rate constant h (mg/mL·min): initial extraction rate	[26,27]
Intraparticle diffusion model $q_t=k_p t^{1/2}$	q_t (mg/g): yield of paclitaxel extracted in the suspension at time t k_P ($mg/g\cdot min^{1/2}$): intraparticle diffusion rate constant	[28]
Fick's law $\ln\left(\frac{Y_s}{Y_s-Y_t}\right)=\ln\frac{\pi^2}{6}+\frac{D_e\pi^2 t}{R^2}$	Y_s: total paclitaxel yield at saturation Y_t: total paclitaxel yield at time t D_e (m^2/s): effective diffusion coefficient R: cell radius (average radius: 42.5×10^{-6} m)	[14,29]
$\ln\frac{C_s}{C_s-C_t}=\frac{K_T A}{V_s}t$ $A=\frac{3m_{plant}}{\rho r_p}$	C_s (mg/mL):saturation concentration of paclitaxel C_t (mg/mL): concentration of paclitaxel at time t A (m^2): total surface area of the particles (cells) m_{plant} (kg): cell weight introduced in the extractor ρ: cell wet density (1,071.43 kg/m^3) r_p: cell size (average radius: 42.5×10^{-6} m) V_s (m^3): volume of solution K_T (m/s): mass transfer coefficient	[30,31]
$Bi=\frac{r_p K_T}{D_e}$	Bi: Biot number	[31]

time (1, 3, 5, 10, and 20 min). During ultrasound-negative pressure cavitation extraction, both ultrasound and negative pressure were introduced and ultrasonic power (180, 250, 380 W), negative pressure (0, −160, and −260 mmHg), and extraction time (1, 3, 6, 8, 10, 12, and 20 min) were varied to find the optimum condition. After extraction, the filtrate was recovered by filtration (filter paper: 185 mm, ADVANTEC) under reduced pressure, concentrated using a concentrator (CCA-1100, EYELA, Japan), and dried under vacuum (at 40 °C, 24 hr, and under −760 mmHg). The paclitaxel content was measured from the dried extract through HPLC analysis. In addition, the quantity of paclitaxel in biomass was obtained through multiple extractions, and the yield of paclitaxel was calculated as follows:

$$\text{Yield (\%)}=\frac{\text{Quantity of paclitaxel in extract}}{\text{Quantity of paclitaxel in biomass}}\times 100 \quad (1)$$

3. Paclitaxel Analysis

An HPLC system (SCL-10AVP, Shimadzu, Japan) and Capell Pak C_{18} (250×4.6 mm, Shiseido, Japan) column were used to determine the paclitaxel content. The mobile phase was distilled water and acetonitrile mixture (65/35-35/65, v/v, gradient mode) and the flow rate was set at 1.0 mL/min. 10 μL of sample was injected and the effluent was detected by UV at 227 nm [15]. Authentic paclitaxel (purity: 97%) was purchased from Sigma-Aldrich and used as a standard. Each sample was analyzed in triplicate.

4. Scanning Electron Microscopy

Changes to the surface of the biomass were observed using scanning electron microscopy (MIRA LMH; Tescan, Czech Republic) [14]. The morphology of the biomass surface was investigated using a 1 mg sample under an accelerated voltage of 10-15 kV at a magnification of 3,000 times.

5. Kinetic Models

The experimental data were applied to the pseudo-first-order model, pseudo-second-order model, and intraparticle diffusion model for the kinetic analysis of the extraction process [25-28]. The effective diffusion coefficient and mass transfer coefficient were determined using Fick's law [14,29-31]. The relative magnitudes of external and internal resistances to mass transfer were determined using Biot numbers. The equations used for estimating the parameters are arranged in Table 1. The parameters in the model were calculated as linear equations based on linear regression analysis through Sigmaplot 10.0 (Systat Software Inc., USA). The effectiveness of the model was evaluated with the determination coefficient (r^2) and root mean squared deviation (RMSD). RMSD is expressed as in Eq. (2).

$$\text{RMSD}=\sqrt{\frac{1}{n}\sum_{i=1}^{n}(\text{experimental}-\text{calculated})^2} \quad (2)$$

where n refers to the number of experimental runs.

RESULTS AND DISCUSSION

1. Comparison of Extraction Methods for Recovery of Paclitaxel from Biomass

In this study, conventional solvent extraction, ultrasonic extraction, negative pressure extraction, and ultrasound-negative pressure

cavitation extraction using methanol were executed to recover paclitaxel from the biomass in one-time extractions. The yields of paclitaxel according to extraction time are presented in Fig. 3. In conventional extraction, the maximum yield of paclitaxel was 77% at 20 min of extraction. In ultrasonic extraction (Fig. 3(a)), the paclitaxel yield was 82, 83, and 90% when the ultrasonic powers was 180, 250, and 380 W, respectively, and the extraction almost reached equilibrium after 10 min. As the ultrasonic power increased, the yield of paclitaxel also increased. Such a phenomenon was because, as the ultrasonic power increased, the cavitation, mechanical effect and thermal effect intensified, thereby improving biomass disruption and mass transfer rate [15-18]. In the negative pressure extraction (Fig. 3(b)), the paclitaxel yield was 87% and 100% at the negative pressures of −160 mmHg and −260 mmHg, respectively. The yield increased as the negative pressure increased and the reaction almost reached equilibrium after 10 min of extraction. The yield increase was due to the presence of the cavitation bubbles generated by the negative pressure and the collapse of these bubbles impacting the biomass to induce cell disruption and ultimately the rapid and uniform dissolving of the active ingredients accumulated in the biomass into the solvent [32-35]. In the ultrasound-negative pressure cavitation extraction (Fig. 3(c)), the paclitaxel yields were 94, 100, 95, 100, 100, and 100% at 180 W/−160 mmHg, 180 W/−260 mmHg, 250 W/−160 mmHg, 250 W/−260 mmHg, 380 W/−160 mmHg, and 380 W/−260 mmHg. The reaction almost reached equilibrium after 3 to 8 min of extraction. As the ultrasonic power and negative pressure increased, the paclitaxel yield also increased. In particular, when the ultrasonic power was 380 W and the negative pressure was −260 mmHg, most of the paclitaxel (>99%) could be recovered from the biomass with a one-time extraction and in a short process time (3 min). On the other hand, in conventional extraction without ultrasound and negative pressure, most of the paclitaxel (~99%) could be recovered from the biomass with a total of four extractions (30 min for each extraction) [14]. Such results were attributed to synergy between ultrasound and negative cavitation. That is, cavitation bubbles formed, grew, and disrupted cell walls effectively, and further hotspots, microjets, and shock waves generated by the collapse of the cavitation bubbles made mass transfer between solvent and solute occur smoothly and increased the paclitaxel extraction efficiency [33-35]. These results are similar to the synergy effect in the ultrasound-negative pressure cavitation extraction of flavonoids from *Flos Sophorae Immaturus* [32].

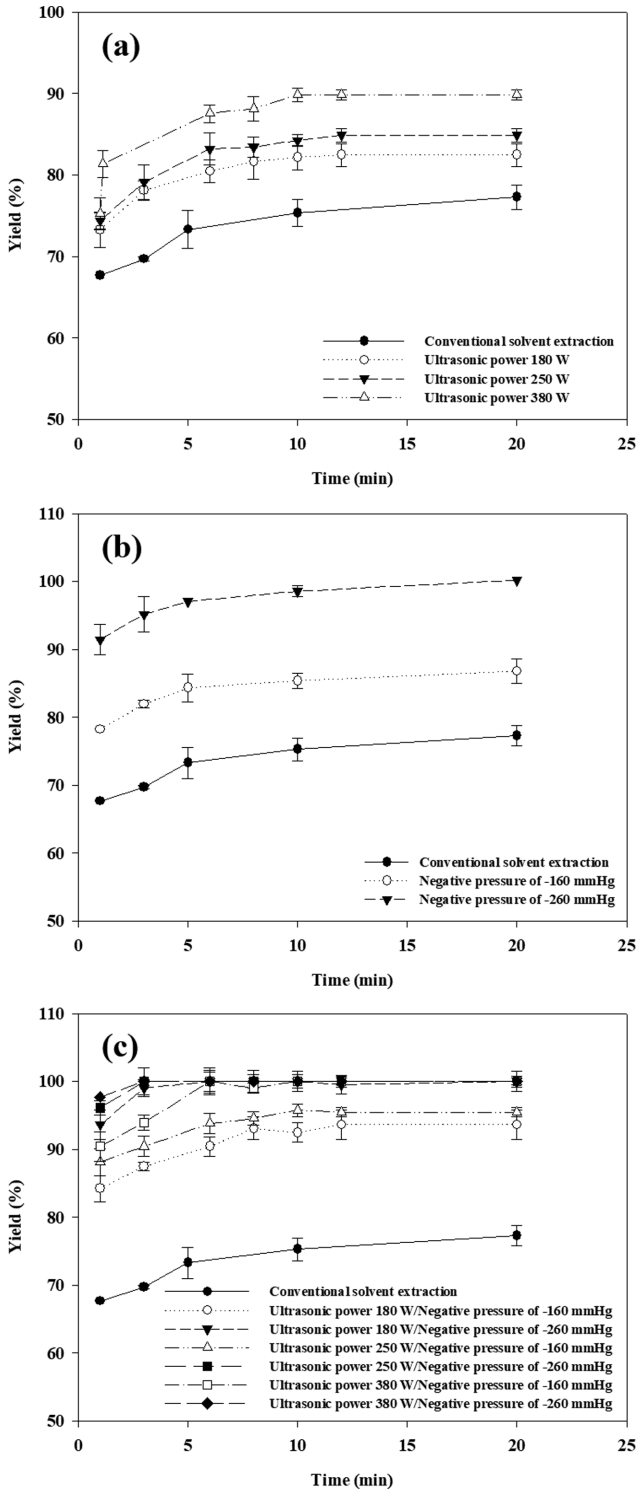

Fig. 3. Effect of operating time on paclitaxel yield during the ultrasonic extraction (a), negative pressure extraction (b), and ultrasound-negative pressure cavitation extraction (c). The biomass/MeOH ratio, stirring speed, and temperature were 1 : 2 (w/v), 500 rpm, and 25 °C, respectively.

2. SEM Analysis

The morphology of the biomass was investigated with SEM. The surface of the biomass before extraction was quite smooth (Fig. 4(a)) but it was somewhat wrinkled after conventional solvent extraction (Fig. 4(b)). In the case of the ultrasonic extraction, as the ultrasonic power became stronger, the surface of the biomass became very rough and shrunken (disrupted) as shown in Fig. 4(c) (180 W), Fig. 4(d) (250 W), and Fig. 4(e) (380 W). This is because increasing the ultrasonic power disrupts more cells due to the central role of the ultrasonic cavitation bubbles themselves and the effect of the bubbles collapsing [36,37]. In the case of negative pressure extraction as shown in Fig. 4(f) (−160 mmHg) and Fig. 4(g) (−260 mmHg), negative cavitation bubbles themselves and the strong impact by the collapse of these bubbles caused a rougher and more shrunken (disrupted) shape compared to the biomass surface before extraction or after conventional extraction. As the

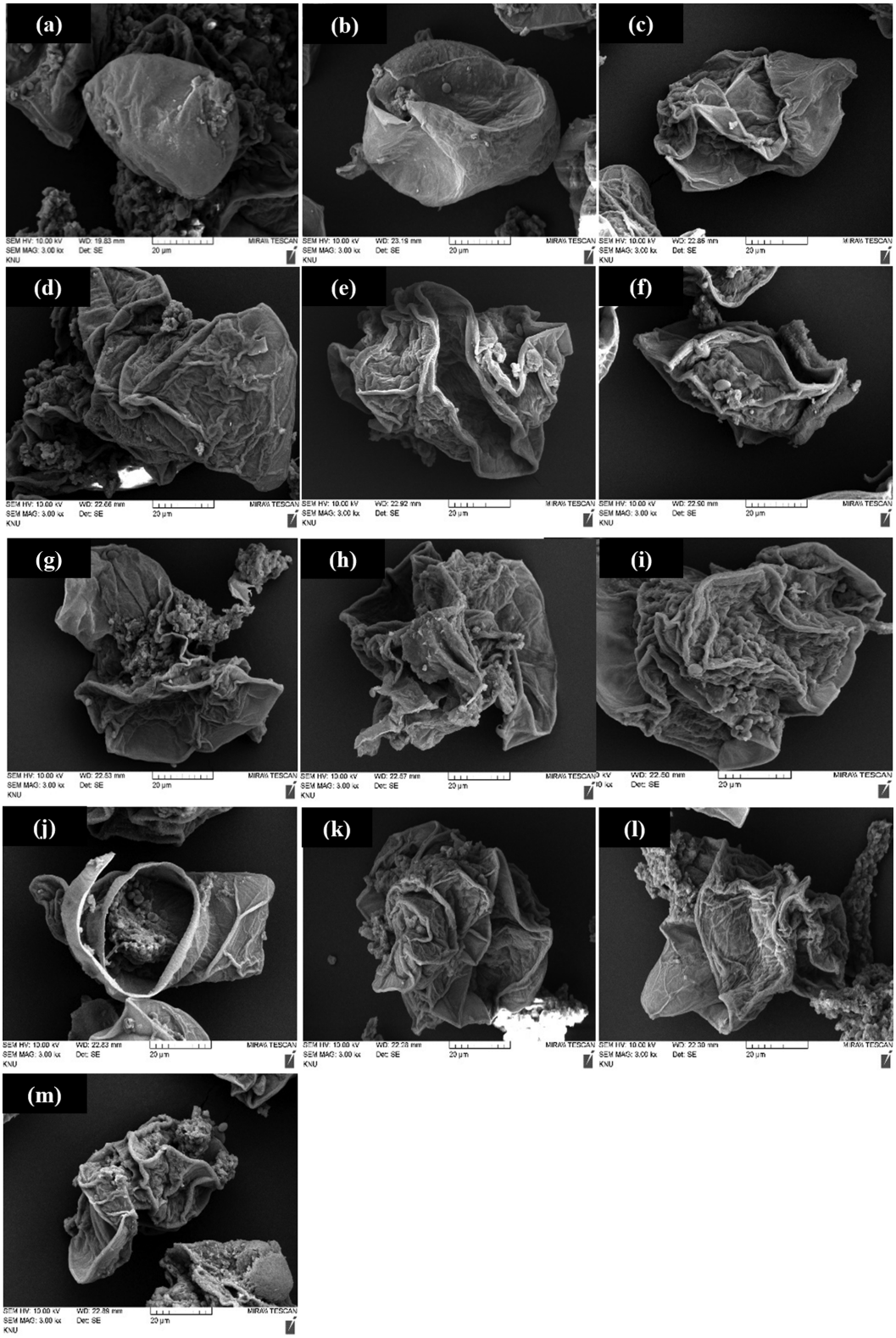

Fig. 4. SEM images of biomass samples treated by ultrasonic extraction, negative pressure extraction, and ultrasound-negative pressure cavitation extraction. (a) Before extraction, (b) Conventional solvent extraction, (c) Ultrasonic extraction (180 W), (d) Ultrasonic extraction (250 W), (e) Ultrasonic extraction (380 W), (f) Negative pressure extraction (−160 mmHg), (g) Negative pressure extraction (−260 mmHg), (h) Ultrasound-negative pressure cavitation extraction (180 W/−160 mmHg), (i) Ultrasound-negative pressure cavitation extraction (180 W/−260 mmHg), (j) Ultrasound-negative pressure cavitation extraction (250 W/−160 mmHg), (k) Ultrasound-negative pressure cavitation extraction (250 W/−260 mmHg), (l) Ultrasound-negative pressure cavitation extraction (380 W/−160 mmHg), (m) Ultrasound-negative pressure cavitation extraction (380 W/−260 mmHg).

negative pressure became more intense, the biomass surface became more wrinkled. This phenomenon was in good agreement with the results of the polysaccharides extraction from *Lentinus edodes* under vacuum conditions [34]. In the case of ultrasound-negative pressure cavitation extraction, the biomass surface was very rough, shrunken, and disrupted after extraction in all the experimental conditions as seen in Fig. 4(h)-(m), which was expected as there was a high paclitaxel yield of 94-100%. However, there was no significant difference in the change of the biomass surface after extraction according to ultrasonic power and negative pressure. In addition, the degree of winkling was greater than in a single application of either ultrasonic extraction or negative pressure extraction. That is, there were enough disrupted surfaces formed so that the paclitaxel accumulated in the cells could be effectively released, resulting in an improved extraction efficiency. From these results, ultrasound-negative pressure cavitation extraction could recover paclitaxel from the biomass more efficiently. The purity (~4.5%) of paclitaxel in the extracts was almost the same in all conditions (data not shown).

Given this, the experimental results for the extraction behavior of paclitaxel from biomass in ultrasound-negative pressure cavitation extraction can be hypothetically explained as shown in Fig. 5. The improvement of extraction efficiency of paclitaxel from the biomass can be explained by synergy between ultrasound and negative pressure (That is, the main mechanism can be interpreted as the synergy between ultrasound-assisted extraction and negative pressure cavitation extraction). Thus, the cavitation bubble itself generated by ultrasound and negative pressure and hotspots, microjets, and shock waves generated by bubble collapse effectively disrupted cells and facilitated mass transfer of paclitaxel, ultimately improving extraction efficiency [36]. Furthermore, the mechanical effect of ultrasound in the ultrasound-negative pressure extraction completely exposes the biomass to a strong ultrasonic field because of the fluidity created by the negative pressure so paclitaxel is more readily released into the extraction solvent [32]. As a result, the ultrasound-negative pressure cavitation extraction can remarkably reduce the large solvent consumption and long extraction time in the conventional extraction.

3. Study of Extraction Kinetics

The extraction data (Fig. 3) were applied to the pseudo-first-order and pseudo-second-order kinetic models to analyze the extraction behavior quantitatively. The comparison of kinetic models revealed that the extraction of paclitaxel from the biomass better fit the pseudo-second-order model in terms of r^2 and RMSD. The plot of t/Ct versus t was drawn using the pseudo-second-order model, and k_2 and C_e were determined from the slope and y-intersect (Table 2). In conventional extraction (without negative pressure and ultrasound), the initial extraction rate (h), extraction rate constant (k_2), and concentration at equilibrium (C_e) were 2.6497 mg/mL·min, 4.3325 mL/mg·min, and 0.7820 mg/mL, respectively. In ultrasonic extraction (without negative pressure), the h (3.4211-6.2500 mg/mL·min), k_2 (4.8414-7.7381 mL/mg·min), and C_e (0.8406-0.8987 mg/mL) increased as the ultrasonic power increased. The h, k_2, and C_e increased by 29-136%, 12-79%, and 7-15%, respectively, compared to the conventional extraction. In negative pressure extraction (without ultrasound), the h (3.9920-6.0132 mg/mL·

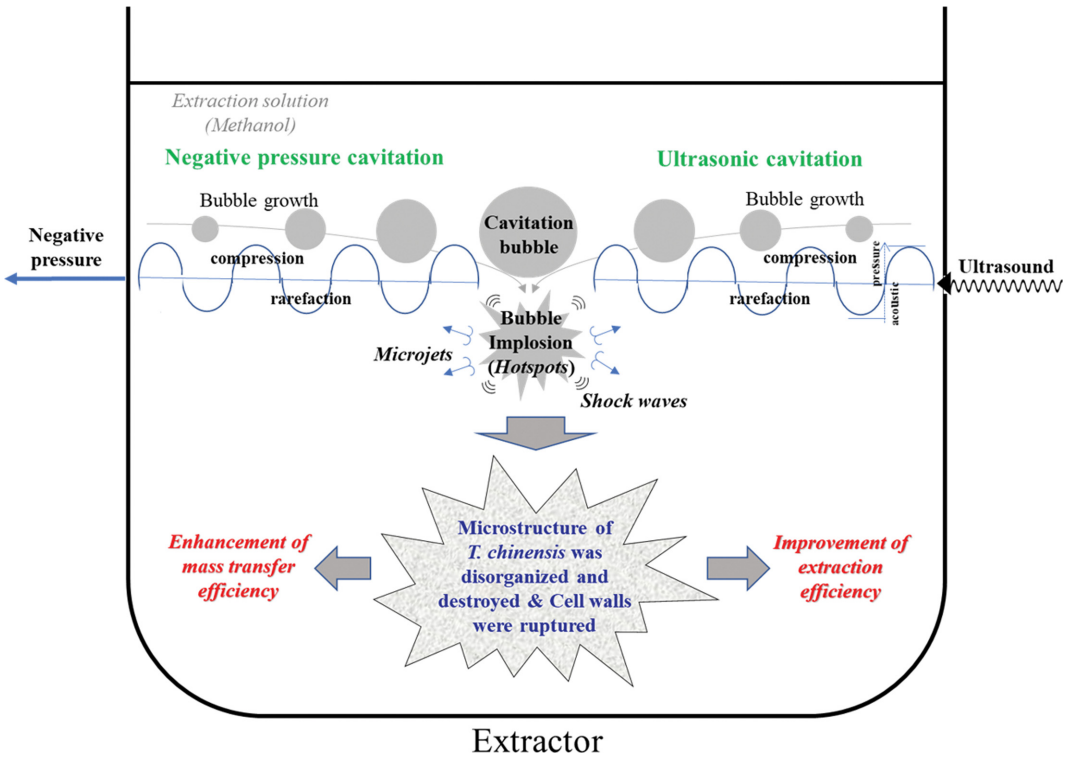

Fig. 5. Hypothetical mechanisms proposed to explain the extraction behavior of paclitaxel from biomass in ultrasound-negative pressure cavitation extraction.

Table 2. Parameters of pseudo-second-order model for the conventional extraction, ultrasonic extraction, negative pressure extraction, and ultrasound-negative pressure cavitation extraction of paclitaxel from biomass at 25 °C

Negative pressure (mmHg)	Ultrasonic power (W)	Parameter	
0	0	h (mg/mL·min)	2.6497
		k_2 (mL/mg·min)	4.3325
		C_e (mg/mL)	0.7820
		r^2	0.9998
		RMSD	0.1100
	180	h (mg/mL·min)	3.4211
		k_2 (mL/mg·min)	4.8414
		C_e (mg/mL)	0.8406
		r^2	0.9997
		RMSD	0.1453
	250	h (mg/mL·min)	5.2882
		k_2 (mL/mg·min)	7.3035
		C_e (mg/mL)	0.8509
		r^2	0.9996
		RMSD	0.1290
	380	h (mg/mL·min)	6.2500
		k_2 (mL/mg·min)	7.7381
		C_e (mg/mL)	0.8987
		r^2	0.9978
		RMSD	0.1957
−160	0	h (mg/mL·min)	3.9920
		k_2 (mL/mg·min)	5.2218
		C_e (mg/mL)	0.8744
		r^2	1.0000
		RMSD	1.5823
	180	h (mg/mL·min)	6.1200
		k_2 (mL/mg·min)	6.8816
		C_e (mg/mL)	0.9430
		r^2	0.9997
		RMSD	0.0718
	250	h (mg/mL·min)	7.0274
		k_2 (mL/mg·min)	7.4612
		C_e (mg/mL)	0.9705
		r^2	0.9997
		RMSD	0.0860
	380	h (mg/mL·min)	10.1626
		k_2 (mL/mg·min)	10.0128
		C_e (mg/mL)	1.0075
		r^2	0.9998
		RMSD	0.0560

min), k_2 (5.2218-5.9126 mL/mg·min), and C_e (0.8744-1.0085 mg/mL) increased as the negative pressure strengthened. This tendency was similar to the study results of other cavitation-based extraction cases [33,34]. When compared to conventional extraction, the h, k_2, and C_e increased by 51-127%, 21-36%, and 12-29%, respectively. In the ultrasound-negative pressure cavitation extraction, the h (6.1200-11.8343 mg/mL·min), k_2 (6.8816-11.6105 mL/mg·min), and C_e (0.9430-1.0096 mg/mL) increased as the ultrasonic power and negative pressure intensified. In addition, the h, k_2, and C_e increased by 131-347%, 59-168%, and 21-29% compared to the conventional extraction. In particular, the increase in h, k_2, and C_e was the largest in ultrasound-negative pressure cavitation extraction. An increase in h and k_2 means an increase in the initial extraction rate and the overall extraction rate. In addition, the increase in C_e

Table 2. Continued

Negative pressure (mmHg)	Ultrasonic power (W)	Parameter	
−260	0	h (mg/mL·min)	6.0132
		k_2 (mL/mg·min)	5.9126
		C_e (mg/mL)	1.0085
		r^2	0.9999
		RMSD	0.0455
	180	h (mg/mL·min)	11.0865
		k_2 (mL/mg·min)	10.9142
		C_e (mg/mL)	1.0079
		r^2	0.9999
		RMSD	0.0368
	250	h (mg/mL·min)	11.4679
		k_2 (mL/mg·min)	11.2465
		C_e (mg/mL)	1.0098
		r^2	0.9999
		RMSD	0.0333
	380	h (mg/mL·min)	11.8343
		k_2 (mL/mg·min)	11.6105
		C_e (mg/mL)	1.0096
		r^2	0.9999
		RMSD	0.0356

means that the solubility of paclitaxel is increased and diffusion is easy due to the synergy of ultrasound and negative pressure [14]. For the recovery of paclitaxel from biomass using cavitation-based extraction, the pseudo-second-order model was suitable, having a large value for r^2 (>0.9978) and a small value for RMSD (<1.5823).

The extraction mechanism was analyzed by the application of the intraparticle diffusion model, which is widely used in the absorption process [14,28]. The plots of the model showed multiple linear characteristics. There were three different parts indicating three extraction stages [14,37]. The first part (Stage I) was a washing step wherein paclitaxel was rapidly moved into the extraction solution from the surface of the biomass. The second part (Stage II) was a diffusion step where paclitaxel slowly moved from the inside to the surface of the biomass. Finally, the third part (Stage III) was an equilibrium step where the extraction almost reached equilibrium [14]. By applying the intraparticle diffusion model, q_t versus $t^{1/2}$ was plotted and presented in Fig. 6. In conventional extraction, the washing step and the diffusion step were clearly distinguished, indicating that the extraction proceeded step by step. On the other hand, in ultrasonic extraction (Fig. 6(a)), negative pressure extraction (Fig. 6(b)) and ultrasound-negative pressure cavitation extraction (Fig. 6(c)), the washing step and the diffusion step

Table 3. Values of the effective diffusion coefficient D_e, the mass transfer coefficient K_T, Biot number Bi obtained for the conventional extraction, ultrasonic extraction, negative pressure extraction, and ultrasound-negative pressure cavitation extraction of paclitaxel from biomass at 25 °C

Negative pressure (mmHg)	Ultrasonic power (W)	$D_e \times 10^{12}$ (m^2/s)	$K_T \times 10^7$ (m/s)	Bi (-)
0	0	1.083	1.428	5.610
	180	1.131	2.149	6.315
	250	1.307	2.194	6.542
	380	1.863	2.298	6.562
−160	0	1.285	2.279	7.546
	180	1.550	2.222	6.100
	250	1.713	2.775	6.893
	380	2.548	3.708	6.192
−260	0	1.377	2.371	7.327
	180	5.143	4.741	4.550
	250	9.916	4.771	2.022
	380	11.528	5.149	1.901

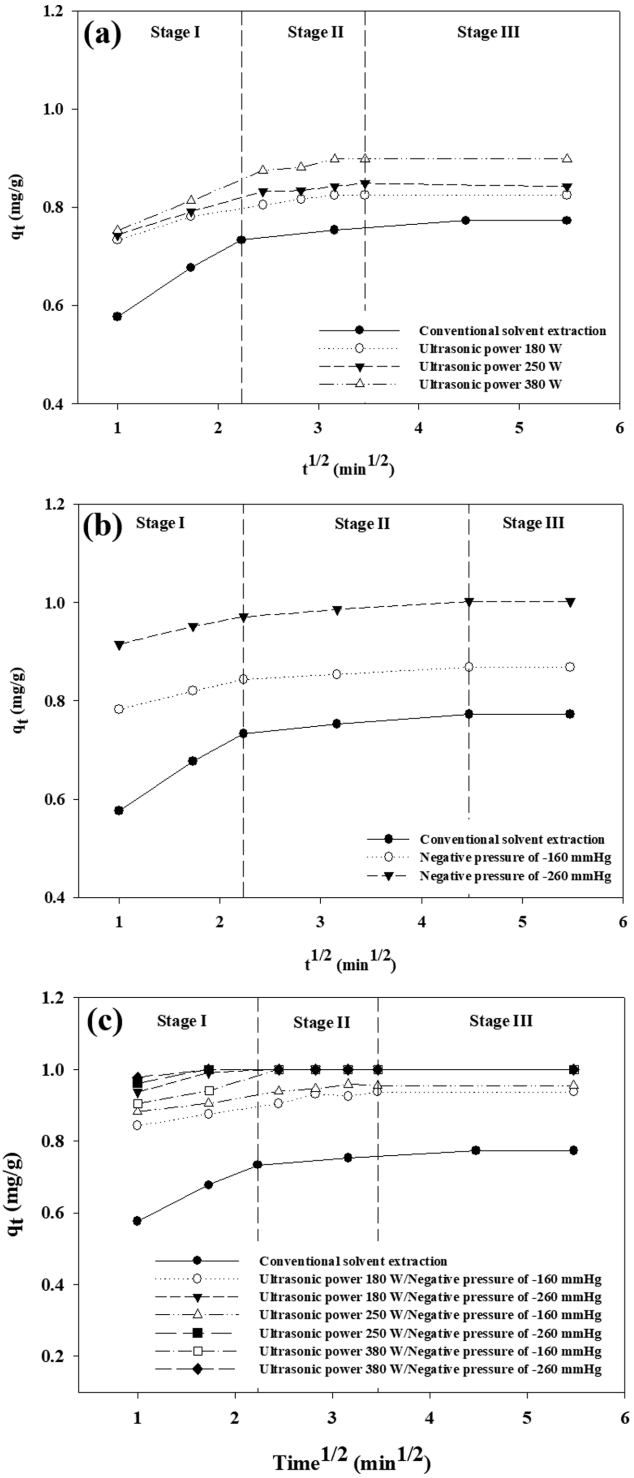

Fig. 6. Intraparticle diffusion plot for the ultrasonic extraction (a), negative pressure extraction (b), and ultrasound-negative pressure cavitation extraction (c) of paclitaxel from biomass at 25 °C.

were not clearly distinguished; therefore, the two extraction steps were performed almost simultaneously. In particular, this phenomenon was more pronounced in the ultrasound-negative pressure cavitation extraction. In all of the extraction methods, the straight line in the diffusion step (Stage II) did not pass the origin, meaning that intraparticle diffusion was not the sole rate-limiting step in the extraction process [14]. The slopes of the linear parts in each stage represent the extraction rate constants. Since the extraction rate constant was smaller in the diffusion step than in the washing step, intraparticle diffusion had more influence on the rate-limiting step. In terms of extraction rate, ultrasound-negative pressure cavitation extraction was more effective than conventional extraction, ultrasonic extraction, and negative pressure extraction, and the extraction rate increased as the ultrasonic power and negative pressure increased. Such combined results are due to synergistic effect and imply that ultrasound-negative pressure cavitation is more effective than ultrasonic cavitation or negative pressure cavitation alone in the extraction process.

4. Determination of Effective Diffusion Coefficient and Mass Transfer Coefficient

The effective diffusion coefficient (D_e), mass transfer coefficient (K_T), and Biot number (B_i) in the conventional extraction, ultrasonic extraction, negative pressure extraction, and ultrasound-negative cavitation extraction are presented in Table 3. D_e in the conventional extraction was 1.083×10^{-12} m^2/s. In ultrasonic extraction, D_e was 1.131×10^{-12}, 1.307×10^{-12}, and 1.863×10^{-12} m^2/s at 180 W, 250 W, and 380 W. This value increased by 4%, 21%, and 72% at 180 W, 250 W, and 380 W, respectively, compared to the conventional extraction. In the negative pressure extraction, D_e was 1.285×10^{-12}, and 1.377×10^{-12} m^2/s at −160 mmHg and −260 mmHg. Compared to the conventional extraction, this value increased by 19% and 27% at −160 and −260 mmHg. In the ultrasound-negative pressure cavitation extraction, D_e was 1.550×10^{-12}, 1.713×10^{-12}, and 2.548×10^{-12} m^2/s and 5.143×10^{-12}, 9.916×10^{-12}, and 11.528×10^{-12} m^2/s, respectively, when the ultrasonic power was 180, 250, and 380 W at −160 mmHg and −260 mmHg. Compared to conventional extraction, this value increased by 43% (180 W), 58% (250 W), and 135% (380 W) and 375% (180 W), 816% (250 W), and 964% (380 W), respectively, at −160 mmHg and −260 mmHg. Furthermore, it increased by 2-94 times and 2-36 times compared to the ultrasonic extraction and negative pressure extraction. The obtained values of D_e (1.083×10^{-12}-11.528×10^{-12} m^2/s) are higher than that for the extraction of andrographolide from *Andrographis paniculate* with water (6.67×10^{-14} m^2/s) and lower than that for the extraction of alkaloids from *Atropa belladonna* with methanol (2.52×10^{-10}-4.79×10^{-10} m^2/s) [14,31].

The K_T for the conventional extraction was 1.428×10^{-7} m/s. In the ultrasonic extraction, the K_T was 2.149×10^{-7}, 2.194×10^{-7}, and 2.298×10^{-7} m/s at 180 W, 250 W, and 380 W. This value increased by 50%, 54%, and 61% at 180, 250, and 380 W, respectively, compared to the conventional extraction. In the negative pressure extraction, the K_T was 2.279×10^{-7} and 2.371×10^{-7} m/s at −160 mmHg and −260 mmHg, respectively. It increased by 60% and 66% at −160 mmHg and −260 mmHg, respectively, compared to the conventional extraction. In the ultrasound-negative pressure cavitation extraction, the K_T was 2.222×10^{-7}, 2.775×10^{-7}, and 3.708×10^{-7} m/s and 4.741×10^{-7}, 4.771×10^{-7}, and 5.149×10^{-7} m/s, respectively, when the ultrasonic power was 180, 250, and 380 W at −160 mmHg and −260 mmHg. Compared to the conventional extraction, this value increased by 56% (180 W), 94% (250 W), and 160%

(380 W) and 232% (180 W), 234% (250 W), and 261% (380 W), respectively, at −160 mmHg and −260 mmHg. The K_T of ultrasound-negative pressure cavitation extraction increased by one to five times and one to four times compared to the single application of ultrasonic extraction and negative pressure extraction. The mass transfer coefficient increased significantly more than the effective diffusion coefficient. This is because the increase in the diffusion coefficient is due to an increase in the thermal energy at higher ultrasonic power and negative pressure, while the increase in the mass transfer coefficient is due to an increase in the diffusion coefficient and a decrease in the viscosity [14,29]. A large Biot number (>1) indicates that the external resistance for mass transfer is negligible due to efficient mixing between solvent and solute and, therefore, internal diffusion is the rate-limiting step [29]. In particular, more severe conditions (−260 mmHg/380 W) led to a smaller Biot number (~1.901), maybe because internal diffusion was greatly improved.

CONCLUSIONS

An ultrasound-negative pressure cavitation extraction method was developed to efficiently recover paclitaxel from plant cell cultures. The yield of paclitaxel in ultrasound-negative pressure extraction was 94-100%, which is superior in terms of recovery rate and operation time compared to ultrasonic extraction and negative pressure extraction. In particular, when the ultrasonic power was 380 W and the negative pressure was −260 mmHg, most of paclitaxel (>99%) could be recovered from the biomass with a one-time extraction and in a short process time (3 min). The extraction kinetics were well explained by the pseudo-second-order model, and intraparticle diffusion played a dominant role in the extraction rate of paclitaxel from the biomass according to the intraparticle diffusion model. As the ultrasonic power and negative pressure increased, the extraction rate constant, the effective diffusion coefficient, and the mass transfer coefficient increased. Internal diffusion was a rate-limiting step with a large Biot number (>1) under all ultrasonic powers (180-380 W) and negative pressures (−160~−260 mmHg), and the internal diffusion was greatly improved at high ultrasonic power and negative pressure (380 W/−260 mmHg).

ACKNOWLEDGEMENTS

This work was supported by the National Research Foundation of Korea (NRF) grant funded by the Government of Korea (MSIT) (Grant Number: 2021R1A2C1003186).

REFERENCES

1. L. Zhu and L. Chen, *Cell. Mol. Biol. Lett.*, **24**, 40 (2019).
2. M. Caillaud, N. H. Patel, A. White, M. Wood, K. M. Contreras, W. Toma, Y. Alkhlaif, J. L. Roberts, T. H. Tran, A. B. Jackson, J. Poklis, D. A. Gewirtz and M. I. Damaj, *Brain Behav. Immun.*, **93**, 172 (2021).
3. Y. S. Jang and J. H. Kim, *Biotechnol. Bioprocess Eng.*, **24**, 529 (2019).
4. M. Ghorbani, F. Pourjafar, M. Saffari and Y. Asgari, *Meta Gene*, **26**, 100800 (2020).
5. T. Sun, Y. Liu, M. Li, H. Yu and H. Piao, *Mol. Cell. Probes*, **53**, 101602 (2020).
6. B. Modarresi-Darreh, K. Kamali, S. M. Kalantar, H. Dehghanizadeh and B. Aflatoonian, *Eurasia J. Biosci.*, **12**, 413 (2018).
7. S. H. Pyo, H. J. Choi and B. H. Han, *J. Chromatogr. A*, **1123**, 15 (2006).
8. H. J. Kang and J. H. Kim, *Process Biochem.*, **99**, 316 (2020).
9. H. W. Seo and J. H. Kim, *Process Biochem.*, **87**, 238 (2019).
10. J. H. Kim, C. B. Lim, I. S. Kang, S. S. Hong and H. S. Lee, *Korean J. Biotechnol. Bioeng.*, **15**, 337 (2000).
11. G. J. Kim and J. H. Kim, *Korean J. Chem. Eng.*, **32**, 1023 (2015).
12. H. J. Kang and J. H. Kim, *Biotechnol. Bioprocess Eng.*, **25**, 86 (2020).
13. H. J. Kang and J. H. Kim, *Korean J. Chem. Eng.*, **36**, 1965 (2019).
14. K. W. Yoo and J. H. Kim, *Biotechnol. Bioprocess Eng.*, **23**, 532 (2018).
15. J. H. Kim, *Korean Chem. Eng. Res.*, **58**, 273 (2020).
16. G. Chen, F. Bu, X. Chen, C. Li, S. Wang and J. Kan, *Int. J. Biol. Macromol.*, **112**, 656 (2018).
17. M. Rakshit and P. P. Srivastav, *J. Food Process. Preserv.*, **45**, e15078 (2020).
18. W. Tang, B. Wang, M. Wang and M. Wang, *J. Appl. Res. Med. Aromat. Plants*, **25**, 100331 (2021).
19. R. Upadhyay, G. Nachiappan and H. N. Mishra, *Food Sci. Biotechnol.*, **24**, 1951 (2015).
20. F. Filianty, *IOP Conf. Ser.: Earth Environ. Sci.*, **443**, 012104 (2020).
21. S. Roohinejad, M. Koubaa, F. J. Barba, R. Greiner, V. Orlien and N. I. Lebovka, *Trends Food Sci. Technol.*, **52**, 98 (2016).
22. A. C. Soria and M. Villamiel, *Trends Food Sci. Technol.*, **21**, 323 (2010).
23. Z. Tan, Q. Li, C. Wang, W. Zhou, Y. Yang, H. Wang, Y. Yi and F. Li, *Molecules*, **22**, 1483 (2017).
24. H. J. Kang and J. H. Kim, *Biotechnol. Bioprocess Eng.*, **24**, 513 (2019).
25. S. Langergren and B. K. Svenska, *Veter. Hand.*, **24**, 1 (1898).
26. L. Rakotondramasy-Rabesiaka, J. L. Havet, C. Porte and H. Fauduet, *Sep. Purif. Technol.*, **54**, 253 (2007).
27. Y. S. Ho, H. A. Harouna-Oumarou, H. Fauduet and C. Porte, *Sep. Purif. Technol.*, **45**, 169 (2005).
28. W. J. Weber and J. C. Morris, *J. Sanit. Eng. Div. Am. Soc. Civ. Eng.*, **89**, 31 (1963).
29. R. Y. Krishnan and K. S. Rajan, *Sep. Purif. Technol.*, **157**, 169 (2016).
30. R. Y. Krishnan, M. N. Chandran, V. Vadivel and K. S. Rajan, *Sep. Purif. Technol.*, **170**, 224 (2016).
31. L. Rakotondramasy-Rabesiaka, J. L. Havet, C. Porte and H. Fauduet, *Sep. Purif. Technol.*, **76**, 126 (2010).
32. G. Wang, Q. Cui, L.-J. Yin, Y. Li, M.-Z. Gao, Y. Meng, J. Li and S.-D. Zhang, *Sep. Purif. Technol.*, **244**, 115805 (2020).
33. D. Panda and S. Manickam, *Appli. Sci.*, **9**, 766 (2019).
34. S. Li, A. Wang, L. Liu, G. Tian and F. Xu, *Food Sci. Biotechnol.*, **28**, 759 (2019).
35. T. Wang, N. Guo, S.-X. Wang, P. Kou, C.-J. Zhao and Y.-J. Fu, *Food Bioprod. Process.*, **108**, 69 (2018).
36. M. Dular, T. Požar, J. Zevnik and R. Petkovšek, *Wear*, **418-419**, 13 (2019).
37. D. Kavitha and C. Namasivayam, *Bioresour. Technol.*, **98**, 14 (2007).